SIZE EFFECT ON THE SHEAR STRENGH OF RC DEEP BEAMS

Kenji Kosa [1], Satoshi Uchida [2], Tsutomu Nishioka [3], and Horoshi Kobayashi [4]

Abstract

To grasp the size effect in reinforced concrete (RC) deep beams with a shear span ratio (a/d) of 1.5, an experiment was conducted using various effective depths (300～1400 mm) as the parameters. Strains within the specimens were measured utilizing dummy reinforcements and acrylic bars. From this experiment, it was found that the relative shear strength decreased as the specimen size became larger due to a relative reduction in the strut width.

1.Introduction

For ordinary RC beams with a shear span ratio (a/d) of 2.5 or more, the presence of size effect which decreases the shear strength as the member size increases has been confirmed. Therefore, based on the loading tests, the size effect is duly taken into account in the equation for calculating the shear strength of a beam.

For ordinary RC deep beams with a/d of below 2.5, Walraven et al. [1)] conducted an experiment using beams with a/d=1.0 and by varying the effective depth (d) from 160mm to 930mm. They found that crack propagation became quicker as the specimen size became larger. But, they did not deal with the internal stress, with no measurement of it using a strain meter or other instruments. For deep beams with a/d=1.5, which is the size frequently employed for actual structures and whose damage pattern varies, little studies have been made to date. Therefore, we conducted an experiment using deep beam specimens with a/d=1.5 and by changing the effective depth (d) in the range of 300～1400 mm (close to a real beam size). Using the measurement results such as strains of reinforcement and concrete, the size effect of deep beams was evaluated.

2. Experimental Program

2.1 Specimens

Table 1 shows the attributes of specimens and the results of compression test. In this experiment, a total of 25 specimens with various parameters, such as a/d (0.5, 1.0. 1.5), shear reinforcement ratio Pw (0.0, 0.4, 0.8%), effective depth d (300-1400 mm) were tested. 19 of them with a/d = 1.5 which is the size frequently adopted for actual structures are shown in this table.

Figure 1 shows reinforcement arrangements and sectional configuration. The left side of the figure shows an example of reinforcement arrangement for Pw=0.0% and the

1) Professor, Dept. of Civil Eng., Kyushu Institute of Technology, Kitakyushu, JP

2) Graduate Student, Dept. of Civil Eng., Kyushu Institute of Technology, Kitakyushu, JP

3) Senior Engineer, Hanshin Expressway Co., Ltd., Osaka, JP

4) Senior Engineer, Hanshin Expressway Co., Ltd., Osaka, JP

Table.1 Attributes of specimens

Specimen No.	Shear span ration a/d	Effective depth d (mm)	Shear reinforcement ration P_w (%)	main reinforcement ration P_t (%)	Compressive strength f'_c (N/mm^2)	Maximum aggregate size Dmax (mm)
B-2	0.5	400	0.0	2.02	36.2	20
B-3			0.4	2.02	36.2	
B-4			0.8	2.02	31.3	
B-6	1.0		0.0	2.02	31.3	
B-7			0.4	2.02	31.3	
B-8			0.8	2.02	37.8	
B-10.1	1.5	300	0.0	2.02	37.0	
B-10.1R				2.02	42.3	
B-10		400		2.02	29.2	
B-10R※				2.02	23.0	
B-10R2				2.02	37.0	
B-10.2		500		2.02	37.0	
B-10.2R				2.02	42.3	
B-10.3		600		2.11	37.8	
B-10.3R※				2.11	31.2	
B-10.3R2				2.11	37.0	
B-13※		800		2.07	31.6	
B-13R※				2.07	24.0	
B-14※		1000		1.99	31.0	
B-15※		1200		1.99	27.0	
B-16※		1400		2.05	27.3	
B-11		400	0.4	2.02	23.0	
B-17※		1000		1.99	28.7	
B-18※		1400		2.05	23.5	
B-12		400	0.8	2.02	31.3	

※ Taken from experiments at PWRI

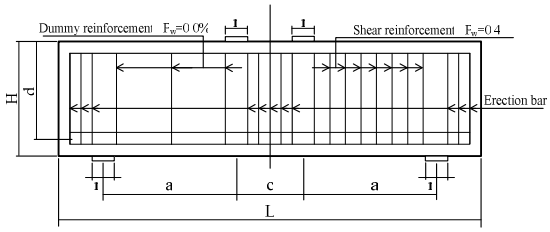

(a) Example of reinforcement arrangement

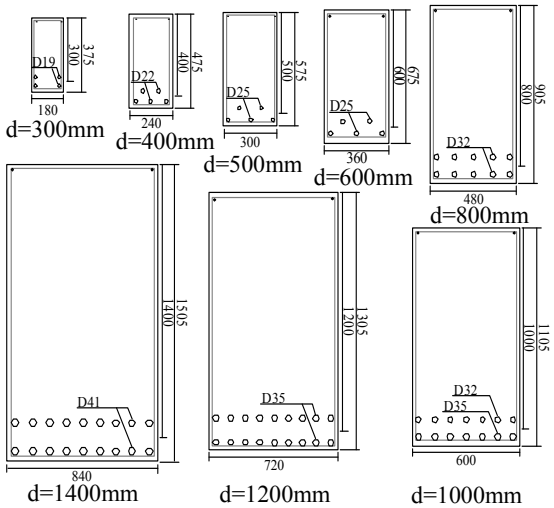

(b) Configuration of section

Fig.1 Configuration of specimens

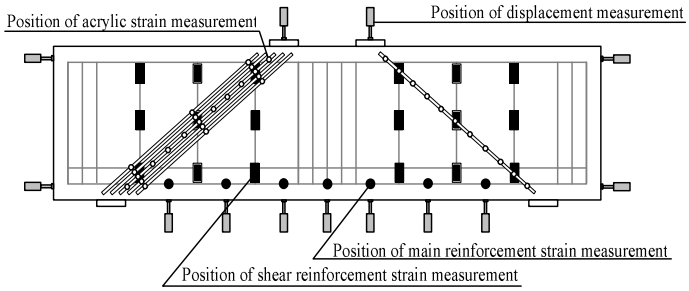

Fig.2 Positions of strain meters and displacement meters

right side for Pw=0.4 and 0.8%. In the case of Pw=0.0% without arrangement of shear reinforcement, dummy reinforcement (Pw=less than 0.05%) is arranged within the shear span for the measurement of strains in the vertical direction. The sectional configuration is identical in all specimens, as shown in Fig. 1(b). Namely, the main reinforcement ratio (about 2.0%) and the maximum aggregate size (Dmax=20 mm) are the same in all specimens. Also, to eliminate the effect of the width of the loading plate and the width of the bearing plate r, r/d is made to 0.25 in all specimens.

2.2 Loading method and measurement items

Using a 30,000 kN loading machine installed at the Public Works Research Institute (PWRI) or a 2000 kN loading machine installed at the Kyushu Institute of Technology, monotonic loads were applied at two symmetrical positions on the specimen. Typical measurement items were five: displacement of a specimen (vertical direction at the bottom end, horizontal direction, and below the loading plate), strain of reinforcement (main reinforcement, shear reinforcement, dummy reinforcement), strain of an acrylic bar, shear displacement, crack width by image analysis.

Figure 2 shows typical installation positions of strain meters and displacement meters. Strain meters on the main reinforcement were installed to measure tensile strain in the horizontal direction caused by flexural deformation. Strain meters on the shear reinforcement and dummy reinforcement were installed to measure tensile strain in the vertical direction mainly around the strut area. As shown in Fig. 2, two displacement meters were installed on the specimen surface at diagonal positions within the shear span to measure shear deformation.

2.3 Measurement of diagonal cracks

The width of cracks within the shear span was measured in the 200x300 mm range at positions of loading plate, strut center, and bearing plate, using a digital camera (600M pixcels). Using image analysis software, the crack width was measured by comparing it with 5x5 mm meshes which were inscribed on the specimen in advance. The crack width was also measured along the diagonal crack, one in each specimen, which was selected for diagonal crack measurement. Two points on both sides of a crack line were measured by matching their shape. Measurements were made at five positions at an interval of 10mm along the crack line and the average values taken.

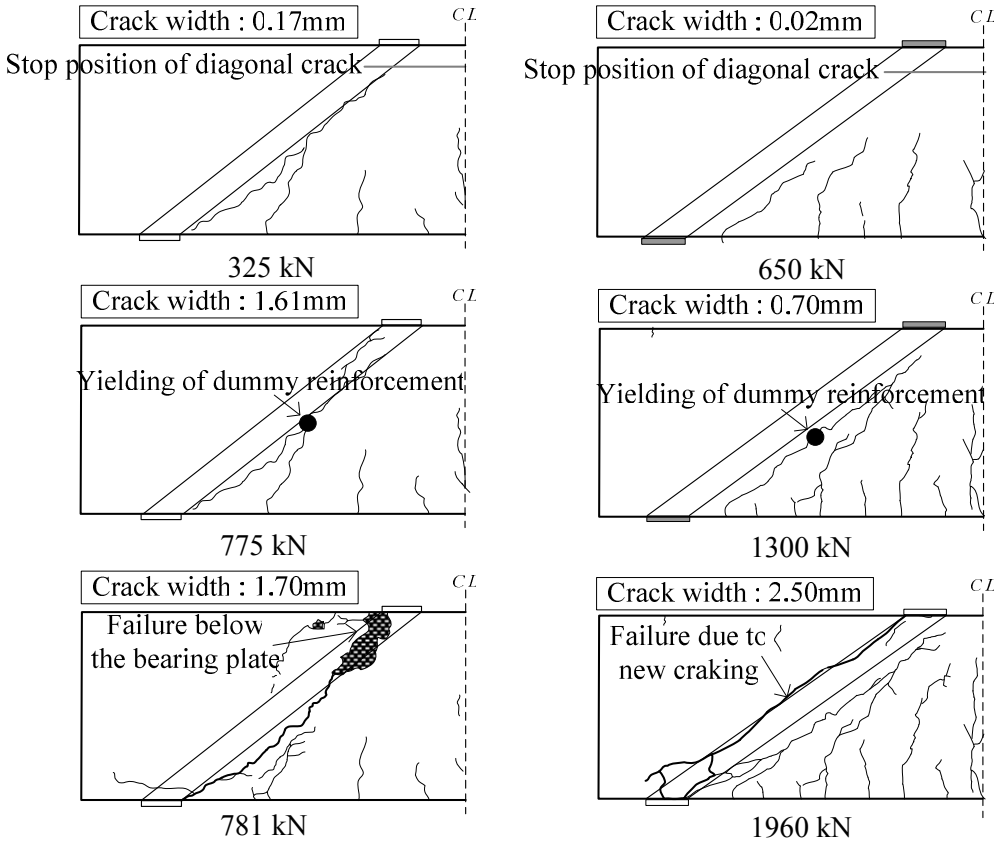

(a) Failure pattern 1 (B-10R2) (b) Failure pattern 2 (B-10.3)

Fig.3 Propagation of cracks

3. Experimental results

3.1 Failure of specimens (a/d= 1.5)

From the loading test of specimens with a/d=1.5, two failure patterns were found: Pattern 1 – failure occurs below the bearing plate; Pattern 2 – failure occurs as a result of propagation of a new crack which starts from below the bearing plate.

(1) Failure pattern 1 (Specimen B-10R2)

Figure 3(a) shows an example of crack propagation of failure pattern 1. In this specimen, shear cracking began under loading of 325kN and propagated up to the stop position shown in the figure. After that, the crack width widened and dummy reinforcement yielded at the position shown in the figure at 775kN. The specimen failed by compression at the position below the bearing plate when the load is 781kN. The crack width widened to 1.70mm.

(2) Failure pattern 2 (Specimen B-10.3)

Figure 3(b) shows an example of crack propagation of failure pattern 2. In this

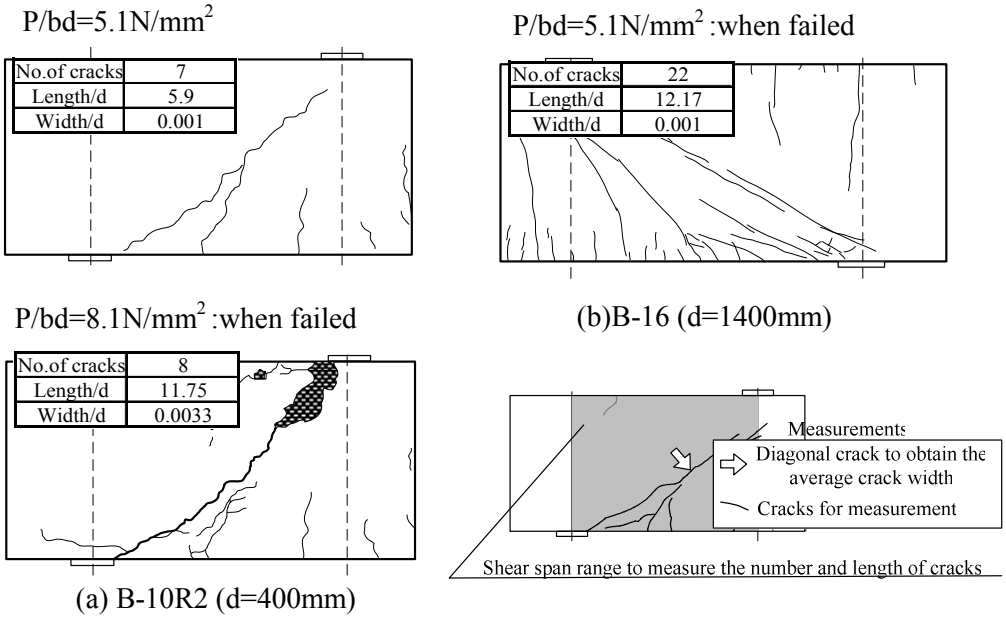

Fig.4 Comparison of crack propagation

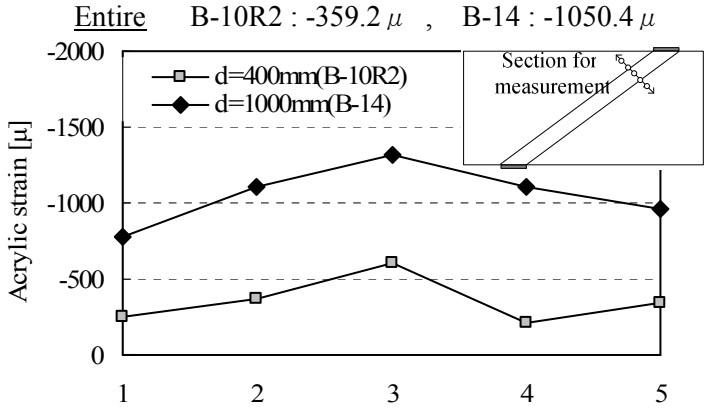

Fig.5 Comparison of strain propagations

specimen, shear cracking started under loading of 650kN and propagated up to the stop position shown in the figure, just like failure pattern 1. After that, the crack width widened. The dummy reinforcement yielded at the position shown in the figure. Then, split cracking started from beneath the bearing plate at 1960kN expanded within the compressive strut and ended in failure. When it failed, the crack width was as large as 2.50 mm.

3.2 Comparison of crack propagation

To find differences in failure pattern by the difference of beam size, crack propagation was compared between a large specimen (Specimen B-16) with d=1400mm

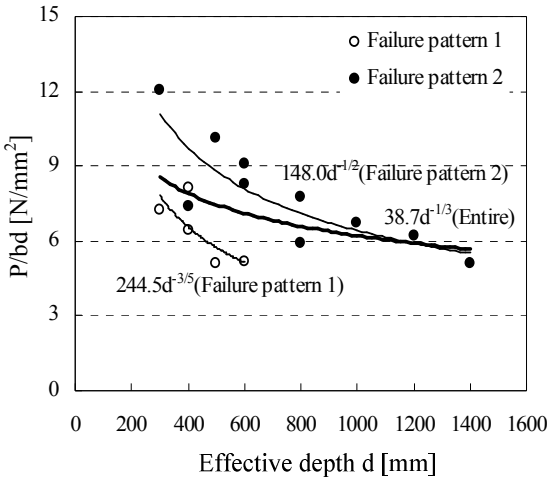

Fig.6 Comparison of shear strength

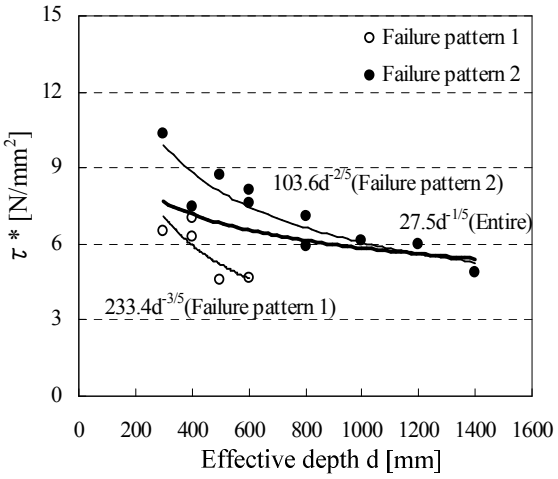

Fig.7 Shear strength with accounting for the effect of concrete

and a small specimen (Specimen B-10R2) with d=400 mm. The results of comparison is shown in Fig. 4. Comparison was made under the same average shear stress which was obtained by dividing the load by bd (width x depth). The number, length, and width of cracks were measured within the shear span indicated by gray color in the figure. As the number of cracks, those that started from the bottom of a specimen were counted. The length and width of cracks were each divided by d and described as the ratio so as to eliminate the effect of member size.

For example, when the two specimens (B-16, B-10R2) were compared under P/bd=5.1N/mm^2 which was equivalent to the maximum shear stress of B-16, crack length/d was 12.17 and 5.90 and the number of cracks 22 and 7, respectively, showing that crack propagation of B-16 is quicker. Specimen B-10R2 (small specimen) failed under the shear stress of P/bd=8.1N/mm^2 and the total crack length/d became 11.75, which is close to that under the maximum loading of B-16 (large specimen). Although the ultimate failure behavior of the specimens is similar because their relative crack length is identical, it can be said that propagation of cracks of a large specimen is quicker than that of a small specimen.

3.3 Comparison of propagation of acrylic strains

In the case of specimens with a/d=1.5, the position beneath the bearing plate failed in the end. Therefore, the distributions of strains below the bearing plate were compared under the same average shear stress. The average shear stress under which comparison was made was P/bd=6.2N/mm^2, which is the shear stress when Specimen B-14 failed.

Figure 5 shows the distribution of strains below the bearing plate. It is known that the average acrylic strain of a large specimen was -1050.4 μ and that of a small specimen -359.2 μ . From this, it can be said that propagation of acrylic strain is also faster in a large specimen than in a small specimen, just like the case of crack propagation.

3.4 Average shear stress

To confirm the presence of the size effect in deep beams with a/d=1.5, the average shear stress was calculated. Figure 6 shows comparison of average shear stress τ which is obtained by dividing the maximum load by the cross section of the member bd (width x depth).

From the figure, it is known that the failure pattern differs even when the effective depth is the same. This is because when a localized force acts due to unevenness of a loading plate or a difference in concrete strength, the resulting failure becomes the pattern 1 type. It is also known that the strength of a beam under failure pattern 1 is smaller than that under failure pattern 2[2]. When attention is paid to each failure pattern, the size effect of $d^{-2/3}$ and $d^{-1/2}$ is caused for failure patterns 1 and 2, respectively. When attention is paid to the entire specimen, the size effect is $d^{-1/3}$. The comparison of shear strength at P/bd takes into account the effect of the member size, but still a difference exists in the compressive strength of concrete. Therefore, the effect of concrete strength was accounted using the ratio of the design strength f'cd to the compressive strength f'ck (Equation (1)).

$$\tau^* = P/bd \left(\frac{f'ck}{f'cd} \right)^{\frac{1}{3}} \quad \cdots\cdots\cdots\cdots \quad (1)$$

Here, τ^* : average shear stress with accounting for the effect of compressive strength

Figure 7 shows the plot of shear strength τ^* with accounting for the effect of compressive strength. It is known from the plot that, just like τ, the shear strength τ^* decreases by $d^{-1/3}$ as the effective depth increases. Therefore, it is considered that when a/d=1.5 the size effect that decreases the shear strength exists.

4. Discussions

It was found in the previous section that when a/d=1.5, diagonal cracks propagate and end in failure due to the fracture below the bearing plate, and that cracks and strains propagate quickly as the member size becomes larger. Therefore, in this section, discussions will be made on 1) rate of crack propagation; 2) failure below the loading plate that occurs in the end.

4.1 Rate of crack propagation

The energy absorption during the propagation of cracks was calculated. It was calculated from the shear displacement because propagation of shear cracks is largely dependent on shear deformation. For this calculation, shear displacement was obtained first using the method in Fig. 8. Then, energy absorption was multipled shear displacement /l (span length) by the average shear stress (P/bd). This process is shown in Fig. 9. For example, energy absorption for P/bd=6.0N/mm^2 of Specimen B-10R2 is the area depicted by gray color and its area is 0.005N/mm^2. In this way, energy absorption under each shear stress was calculated.

Figure 10 shows the development of energy absorption of Specimen B-10R2

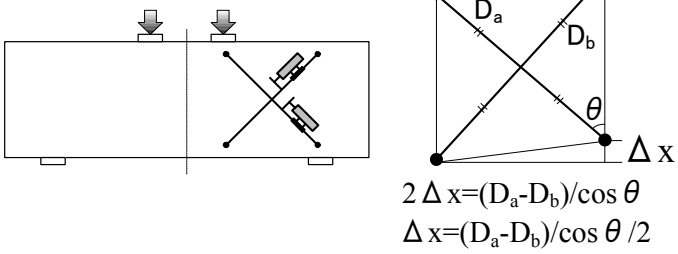

Fig.8 Calculation of shear displacement

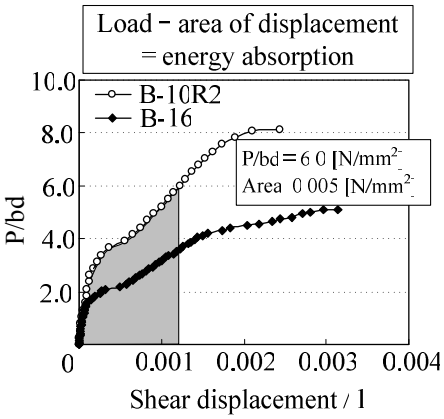

Fig.9 Calculation of energy

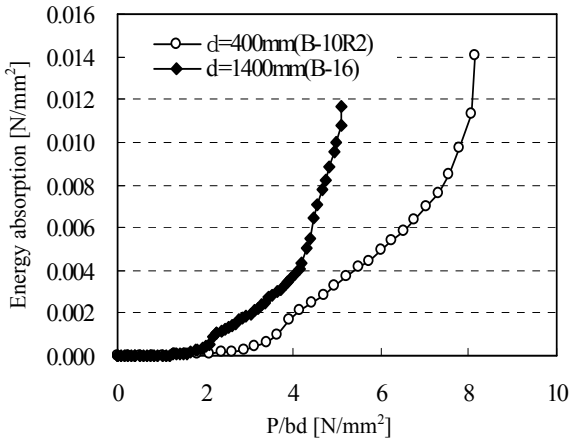

Fig.10 Development of energy absorption

(small specimen) and B-16 (large specimen). It is known from the figure that energy absorption of B-16 is always larger than that of B-10R2 when the same average shear stress acts. Because of this, crack propagation is always quicker in large specimens than in small specimens.

4.2 Failure below the loading plate

In our separate research[2], we found that the vertical component P' of compressive force acting on the strut and the load applied P are approximately the same when a/d=1.5, as shown in Fig. 11. P' is influenced by the area of compressive stress distribution (A) shown in the figure. **A** is determined by the compressive stress and the strut width Wp.

Therefore, we focused on the acting stress and Wp. The strut width which is necessary for the calculation of Vc was obtained from the shape of compressive strain of an acrylic bar at the time of 0.95Pmax which is close to the ultimate state.[3]

To compare the acting stresses at the time of failure, the acting shear stress τ of large and small specimens was estimated. As shown in Fig. 11, the stress distribution area A was divided by Wp and then average of the stress distribution was taken. Figures

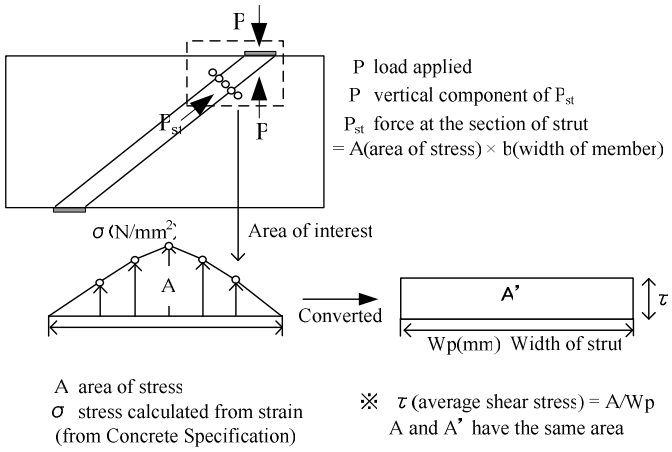

Fig.11 Calculation of P'

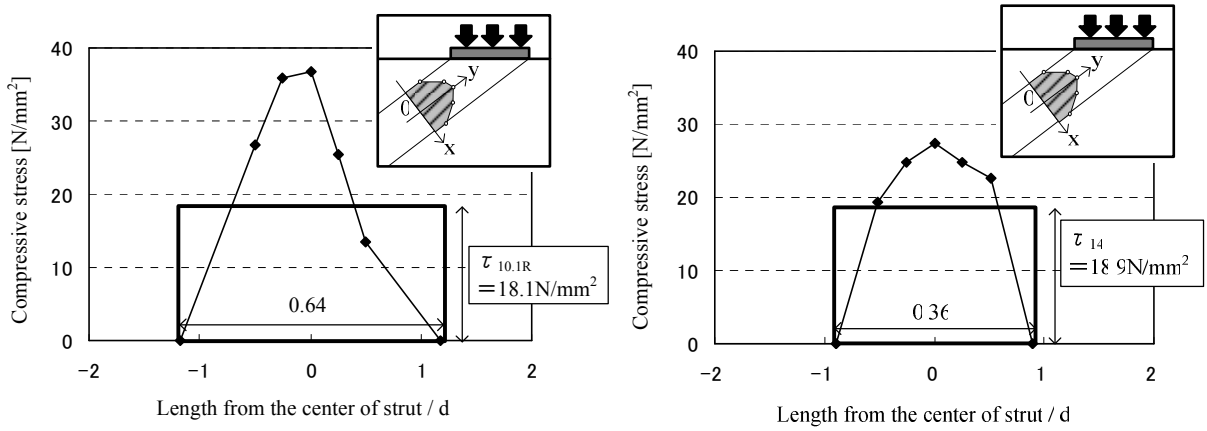

(a) Specimen B-10.1R (d=300mm) (b) Specimen B-14 (d=1000mm)

Fig.12 Distribution of compressive stress

12(a) and 12(b) show the stress distribution of Specimen B-10.1R (d=300mm) and Specimen B-14 (d=1000mm).

To make it dimensionless for comparison, Wp was divided by the loading width d and showed as the dimensionless ratio in the figure. It is known from the figure that the maximum shear force ($\tau_{10.1R}$) of Specimen B-10.1R is 18.1N/mm^2, and that the maximum shear force (τ_{14}) of Specimen B-14 is 18.9N/mm^2.

As seen, the acting shear stress was roughly the same when specimens failed below the loading plate, indicating that Wp has a significant influence on the size effect. Figure 13 shows the results of comparison. It is seen that as the relative depth becomes larger, the apparent strut width decreases by $d^{-1/2}$ for failure pattern 1, $d^{-2/3}$ for failure pattern 2 and $d^{-1/3}$ for the entire specimen. It can be said that failure becomes localized as the specimen size becomes larger.

4.3 Effect on the shear resistance

As mentioned earlier, propagation of cracks is quicker and failure is localized as the specimen size becomes larger in case of specimens with a/d=1.5. To investigate if

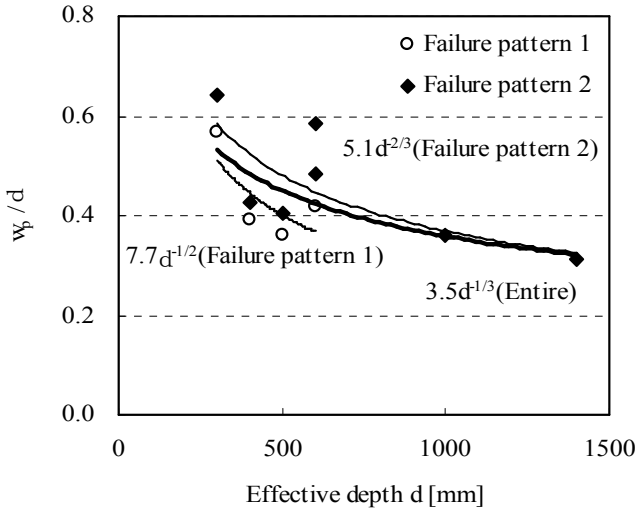

Fig.13 Comparison by making W_p dimensionless

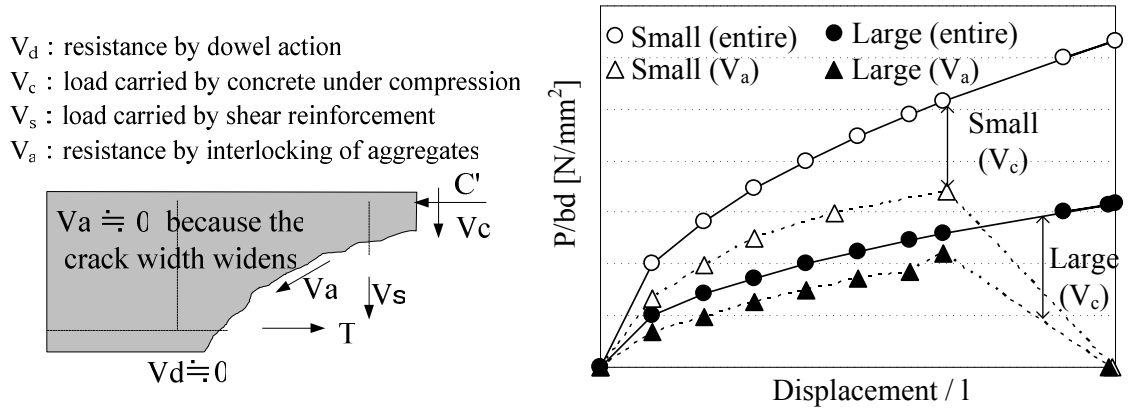

(a) Components of shear resistance for a/d = 1.5 (b) Estimation of shear resistance

Fig.14 Schematic of shear resistance for the case of a/d = 1.5

this nature has an effect on the shear strength of a deep beam, the authors proposed a shear resistance model for beams with a/d=1.5, which is shown in Fig.14 [2]. According to this model, the shear resistance during the propagation of cracks is primarily governed by the combination of Va and Vc. However, in the ultimate state, Va becomes smaller as the crack width widens and the shear resistance is governed by Vc.

If this concept is applied, shear resistance Va of a large specimen becomes small compared with that of a small specimen because crack propagation is quicker in the former specimen, which is shown in Fig. 14(b). Similarly, shear resistance Vc of a large specimen is also small because failure occurs in a localized area in the ultimate state. Because of a combination of these two phenomena which decrease the shear resistance, the shear resistance of a specimen with a/d=1.5 becomes relatively small as the specimen size becomes larger.

5. Conclusions

The following conclusions were drawn from the study on the size effect of deep beams with a/d=1.5 (shear span ratio).

(1) When failure behavior of large and small specimens were compared under the same average shear stress, the crack length /d became 12.17 in a large specimen (B-16) (d=400mm) and 5.90 in a small specimen (B-10R2) (d=400mm). It means that crack propagation is quicker in a large specimen than in a small specimen.

(2) From the investigation of the size effect, two types of failure patterns were found. The size effect which decreases the shear stress by $d^{-1/3}$ was found to exist as a whole.

(3) From the investigation of the strut width of specimens with d=300～1400mm, it was found that the apparent strut width decreased by $d^{-1/3}$ as the member size increased, Then, a localized failure occurred and the relative shear strength decreased.

References

1) J. Walraven et al., Size Effects in Short Beams Loaded in Shear, ACI Structural Journal, pp. 585-593, Sept.-Oct., 1994.

2) T. Wakiyama, K. Kosa, T. Nishioka, H. Kobayashi, Effect in the Failure Behavior of Deep Beams, Proc. of JCI, Vol. 26, No.2, pp. 1015-1020, June 2005 (in Japanese).

3) K. Kosa, Y. Umemoto, T. Nishioka, and H. Kobayashi, Experimental Study on the Damage Pattern of Deep Beams, Proc. of Structural Engineering, Vol. 51A, pp. 1283-1290, April, 2005 (in Japanese).

4) H. Noguchi and M. Ochiai, Study of Shear Resistance Mechanism of Reinforced Concrete Beams, Proc. of JCI, Vol. 1, pp. 441-444, June 1980 (in Japanese).